ChemComm

Accepted Manuscript

This article can be cited before page numbers have been issued, to do this please use: P. Zhang, Y. Wang, K. Qiu, Z. Zhao, R. Hu, C. He, Q. Zhang and H. Chao, *Chem. Commun.*, 2017, DOI: 10.1039/C7CC07776A.

ROYAL SOCIETY OF CHEMISTRY

rsc.li/chemcomm

View Article Online
DOI: 10.1039/C7CC07776A

Journal Name

COMMUNICATION

Received 00th January 20xx,

Accepted 00th January 20xx

DOI: 10.1039/x0xx00000x

www.rsc.org/

NIR phosphorescent osmium(II) complex as lysosome tracking reagent and photodynamic therapeutics†

Pingyu Zhang*[a], Yi Wang[a], Kangqiang Qiu[a,b], Zhiqian Zhao[a], Rentao Hu[a], Chuanxin He[a], Qianling Zhang*[a] and Hui Chao*[a,b]

A novel near infrared (NIR) phosphorescent osmium complex (Os1) was developed for lysosome tracking and photodynamic therapy. Its NIR photophysical property, cellular imaging and phototoxicity have advantages over its ruthenium analogue (Ru1).

Metal coordination complexes have attracted a great interest in the fields of chemical sensors and bioimaging because they possess tunable and intense emission, long emission lifetimes, large Stokes shifts, and high photostability.[1] In this regard, Ru(II) and Ir(III) complexes are particularly promising because of their excellent photophysical and electrochemical properties, which can also be systematically modulated to a significant extent by changing the ligands, as well as due to their robust structure.[2] These metal complexes have emerged as promising alternative choices to organic dyes as diagnostic probes and tracking agents for diseases.[2e]

Whilst osmium complexes featuring labile ligands have been the focus of numerous important studies as anti-cancer agents,[3] few osmium polypyridyl complex was examined to date in the context of their capacity as cellular imaging probes.[4] Although the emission quantum yields and lifetimes of Os(II) polypyridyl complexes tend to be lower, they share many of the photophysical advantages of their Ru(II) analogues. Firstly, Os(II) polypyridyl complexes typically exhibit emission maxima in the NIR spectral region, strongly coincident with the biological optical window.[5] Secondly, because of their increased crystal field splitting, the osmium d–d states cannot be accessed by thermal crossover from its excited triplet state, as is the case for ruthenium.[6]

Near-infrared (NIR) fluorophores with emission wavelengths in the region of 650–900 nm can markedly decrease light scattering and background absorption, minimize photodamage to biological samples, and can also improve tissue depth penetration.[7] Potential uses span from optoelectronic/solar energy materials, to research imaging probes and, to fluorescence guided precision surgery, such as photodynamic therapy.[8] However, most of the available NIR fluorescent probes are mainly limited to organic dyes,[9] semiconductor quantum dots (QDs)[10], metal-organic framework (MOF) nano-particles[8d] and lanthanide upconversion nanophosphors,[11] these compounds have several significant limitations such as poor photostability, larger size and small Stokes shift, etc.[12]

Compared with these NIR fluorescent probes, Os(II) complexes offer advantages of long MLCT absorption, high photostability and excellent NIR emission.[13] Recently, McFarland and co-workers reported three osmium-based photosensitizers, $[Os(biq)_2(phen)](PF_6)_2$ (TLD1822, biq = 2,2′-biquinoline, phen = 1,10-phenanthroline), $[Os(biq)_2(IP)](PF_6)_2$ (TLD1829, IP = imidazo[4,5-f][1,10]phenathroline) and $[Os(biq)_2(dppn)](PF_6)_2$ (TLD1824, dppn = benzo[i]dipyrido[3,2-′:2′,3′-c]phenazine). These photosensitizers were panchromatic, activatable from 200 to 900 nm and had strong resistance to photobleaching. *In vitro* studies showed photodynamic therapy efficacy with both red and NIR light in normoxic and hypoxic conditions, which translated to good *in vivo* efficacy of TLD1829 in a subcutaneous murine colon cancer model.[5]

Herein, we designed a pair of Ru(II) and Os(II) analogues (Fig.1) and studied their photophysics, cellular imaging and photodynamic therapy. The results suggested that **Os1** exhibited NIR phosphorescence emission (700-850 nm) and interestingly accumulated in lysosome, allowing for NIR imaging. However, **Ru1** showed red luminescence (550-700 nm) in mitochondria. Furthermore, **Os1** showed obvious photocytotoxicity to the cancer cells after NIR light irradiation. This novel Os(II) complex is the first report for NIR lysosome tracking and NIR photodynamic therapy.

The syntheses of **Ru1** and **Os1** were described in the experimental section and Fig. S1 in the supporting information. They were characterized by the MS, NMR and elemental analysis (Figs. S2-S8). The wavelength of the MLCT absorption of **Ru1** was 459 nm and its red phosphorescence of **Ru1** emitted from 550 to 700 nm in the PBS

[a] *Shenzhen Key Laboratory of Functional Polymer, College of Chemistry and Environmental Engineering, Shenzhen University, Shenzhen, 518060, P. R. China E-mail: p.zhang6@szu.edu.cn; zhql@szu.edu.cn*
[b] *School of Chemistry, Sun Yat-Sen University, Guangzhou, 510275, P. R. China ceschh@mail.sysu.edu.cn*
†Electronic Supplementary Information (ESI) available: Experimental details, MS and NMR spectra and figures referenced throughout the text.
See DOI: 10.1039/x0xx00000x

View Article Online
DOI: 10.1039/C7CC07776A

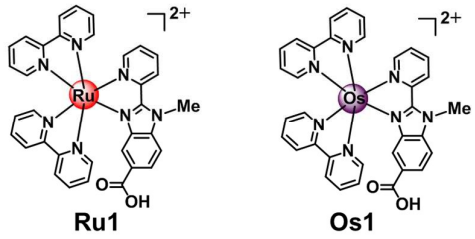

Fig. 1. The chemical structures of **Ru1** and **Os1**.

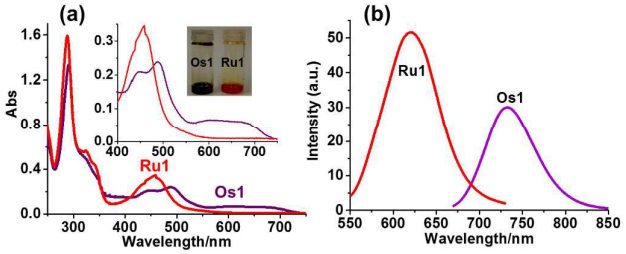

Fig. 2. (a) UV-vis and (b) emission spectra of **Ru1** and **Os1** (20 μM) in the PBS solution (with 1% DMSO); the wavelengths of excitation of **Ru1** and **Os1** were 465 nm and 633 nm, respectively.

solution, whereas **Os1** showed the MLCT absorption at 488 nm and 683 nm, and exhibited NIR emission between 700-850 nm (Fig. 2). This is probably due to strong spin-orbit coupling induced by heavy Os(II), then the spin-forbidden ^{3}MLCT absorption bands were seen in the NIR region.[13b] In contrast to its Ru(II) analogue and most of Ir(III) complexes,[14] **Os1** exhibited longer wavelength of emission, which is usefully situated inside the biological window and out of the range of cellular autofluorescence. In addition, both **Ru1** and **Os1** were highly stable in the cell culture medium (RPMI-1640) for 72 h (Fig. S9).

Due to their strong phosphorescence properties, the cellular distribution in A549 cancer cells was investigated by confocal laser scanning microscopy. As shown in Fig. 3, the colocalization experiment of **Ru1** with MitoTracker® Green (MTG) in the A549 cells demonstrated high overlap, with a Pearson's colocalization coefficient of 82.3% (Fig. 3a). Meanwhile, little colocalization for **Ru1** and LysoTracker® Green (LTG) or Hoechst 33258 was observed (Fig. 3b and Fig. S10). However, **Os1** was found to have high overlap with lysosomes, with a Pearson's colocalization coefficient of 87.6%, but few in either nucleus or mitochondria (Fig. 3c,d and Fig. S10). Furthermore, for **Ru1**, the inductively coupled plasma mass spectrometry (ICP-MS) results revealed that the level of cellular Ru in the mitochondria (80.3%) was much higher than that in the cell membrane, lysosomes and nucleus. For **Os1**, we found that most of cellular Os were located in the lysosomes and very few Os was in the nucleus, membrane or mitochondria (Fig. S11).

To explore the application of **Ru1** and **Os1** as cellular dyes, the photostabilities of the complexes were examined in comparison to MTG and LTG. Figs. S12, S13 showed that the fluorescence intensities of MTG and LTG decreased obviously after irradiation of 488 nm light for 30 min. The phosphorescence intensities of **Ru1** and

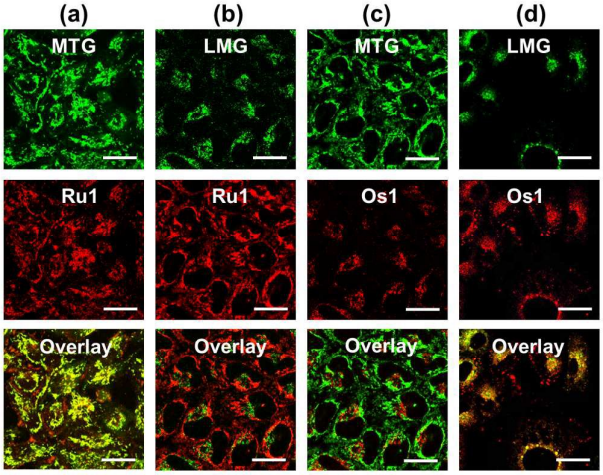

Fig. 3. Confocal images of the A549 cells colabeled with **Ru1** or **Os1** (20 μM, 4 h) in the RPMI-1640 medium (with 1% DMSO) and (a, c) MitoTracker® Green (MTG, 100 nM, 30 min), and (b, d) LysoTracker® Green (LTG, 100 nM, 30 min). **Ru1**: λ_{ex} = 458 nm, λ_{em} = 600±30 nm; **Os1**: λ_{ex} = 561 nm, λ_{em} = 720±30 nm; MTG/LTG: λ_{ex} = 488 nm, λ_{em} = 520 ± 30 nm; Hoechst 33258: λ_{ex} = 405 nm, λ_{em} = 450 ± 30 nm; Scale bar: 20 μm.

Os1 remained mostly unchanged after photobleaching in aqueous solution and living A549 cancer cells. In addition, we observed that **Os1** still showed strong phosphorescence in lysosome after 12 h and 48 h incubation (Fig. S14). These results indicated that **Ru1** and **Os1** exhibited outstanding photostabilities and were suitable for long-time tracking of lysosomes in the living cells.

It was interesting to find out that **Ru1** and **Os1** targeted different cellular organelles. **Ru1** and **Os1** have the same ligands and charge. The difference between them lies in the metal center. We firstly thought that this is due to their abilities in responding to biological pH. Thus, the emission intensities of **Ru1** and **Os1** were measured at various pH values ranging from 4.11 to 10.48 in the PBS solution. The phosphorescence intensity exhibited no obvious change in these pH values for both **Ru1** and **Os1** (Fig. S15). Then we speculated that the hydrophilicity influenced by metal center was responsible for the different targets of **Ru1** and **Os1**. To determine the hydrophilicities of **Ru1** and **Os1**, the n-octanol/water partition coefficients (log P) were measured. The results showed that **Os1** was more lipophilic, with a log P of -1.24±0.11. However, **Ru1** was more hydrophilic, with a log P of -2.23±0.28. Previous report suggested that difference in log P might make a difference in the cellular targets in the living cells.[14]

Next we measured whether O_2 affects the phosphorescence intensities of **Ru1** and **Os1**. The result showed that **Ru1** and **Os1** had much stronger phosphorescence under N_2 than that in the air (Fig. S16), and higher Φ_{em} under N_2 environment (0.047 for **Ru1** and 0.012 for **Os1**, Table 1). The emission lifetimes of **Ru1** and **Os1** were longer under N_2 than (89 ns for **Ru1**, 72 ns for **Os1**) that in the air (43 ns for **Ru1**, 24 ns for **Os1**) (Table 1 and Fig. S17). As

View Article Online
DOI: 10.1039/C7CC07776A
Journal Name COMMUNICATION

expected, the presence of oxygen had a great influence on the phosphorescence and lifetimes of **Ru1** and **Os1**.

Table 1. Photophysical data for **Ru1** and **Os1**.

Complex	λ_{abs}[nm](ε[$M^{-1}cm^{-1}\times10^4$])[a]	λ_{em}[nm][a]	Φ_{em}[b]		Lifetimes τ[ns][c]		$\Phi(^1O_2)$[d]	
			Air	N_2	Air	N_2	465 nm	633 nm
Ru1	459 (0.67)	619	0.016	0.047	43	89	0.10	0.001
Os1	488 (0.50); 683 (0.14)	736	0.009	0.012	24	72	0.003	0.05

[a] Absorption and emission spectra recorded in H_2O (with 1% DMSO) at 310 K; [b] Φ_{em}, luminescence quantum yield in H_2O (with 1% DMSO); [c] τ, lifetime, determined in H_2O (with 1% DMSO). [d] $\Phi(^1O_2)$, quantum yields for $^1O_2$ determined under 465 nm and 633 nm light irradiation, respectively. $Ru(bpy)_3]^{2+}$ was used as a standard photosensitizer (Φ_{em} = 0.028, $\Phi(^1O_2)$ = 0.22 in water[15])

$^1O_2$ generation by **Ru1** and **Os1** upon 465 nm (blue) and 633 nm (red) light irradiation was detected by electron paramagnetic resonance (EPR) spectroscopy using 2,2,6,6-tetramethylpiperidine (TEMP) as the spin-trap. As illustrated in Fig. S18, the characteristic triplet-of-triplets (3450-3510 G) for the 2,2,6,6-tetramethylpiperidine-1-oxyl radical was observed in the **Ru1** sample after 465 nm light irradiation and **Os1** sample after 633 nm light irradiation. No $^1O_2$ signal was observed either in the **Ru1** sample upon 633 nm light irradiation or in the **Os1** sample upon 465 nm light irradiation. $\Phi(^1O_2)$ of **Ru1** and **Os1** upon irradiation were determined (the quenching of the absorbance of ρ-nitrosodimethyl aniline (RNO) by a trans-annular peroxide adduct formed by $^1O_2$ and an imidazole derivative[16]) as 0.10 (**Ru1**, 465 nm light) and 0.05 (**Os1**, 633 nm light), respectively (Fig. S19 and Table 1). $\Phi(^1O_2)$ of **Ru1** upon 633 nm light irradiation and **Os1** upon 465 nm light irradiation were much lower.

The phototoxicities of **Ru1** and **Os1** towards various kinds of cells were further studied (Fig. 4 and Table S1). After treatment with different concentrations of **Ru1** and **Os1** for 4 h, and incubated without non-complexes medium for another 44 h. The result showed that **Ru1** and **Os1** were no cytotoxicity (IC_{50} = 425 and 406 μM, respectively) in the dark. The cancer cells exhibited no loss of viability after being irradiated with these lights in the absence of the Ru/Os complexes (control + irradiation, Fig. S20). However, **Ru1** was highly toxic to A549 cancer cells (IC_{50} = 12.3 μM) after 465 nm light irradiation (4.8 mW/cm^2, 1 h) but not 633 nm light irradiation (11.1 mW/cm^2, 3 h, IC_{50} = 442 μM). Interestingly, **Os1** showed great phototoxicity after 633 nm light irradiation (IC_{50} = 31.7 μM) and its phototoxicity index upon 633 nm (PI_{633} = IC_{50} (dark) / IC_{50} (633nm light)) was 12.8 (Table S1). **Ru1** and **Os1** also showed toxicity towards HeLa and Hep-G2 upon irradiation but almost non-toxicity to MRC-5 normal cells both in the dark and upon irradiation (IC_{50} > 100 μM, Table S1). And the phototoxicity of **Os1** was more excellent than the reported Os(II) complexes (TLD1822, TLD1824 and TLD1829)[5a]. Under the same experimental conditions, 5-ALA (5-amino-levulinic acid) and cisplatin displayed almost no phototoxicity.

To demonstrate that **Ru1** and **Os1** can produce cellular $^1O_2$ after light irradiation, A549 lung cancer cells were incubated with **Ru1** and **Os1** and the fluorescence probe 2,7-dichlorodihydro-fluorescein diacetate (DCFH-DA). The cells treated with DCFH-DA and the complexes in the dark showed no enhancement of fluorescence (Fig. S21). In contrast, a significant increase in fluorescence from DCFH-DA was observed in the cells treated with **Ru1** upon 465 nm light irradiation or **Os1** upon 633 nm light irradiation. However, the cells treated with **Ru1** upon 633 nm irradiation or **Os1** upon 465 nm irradiation showed weak fluorescence (Fig. S21).

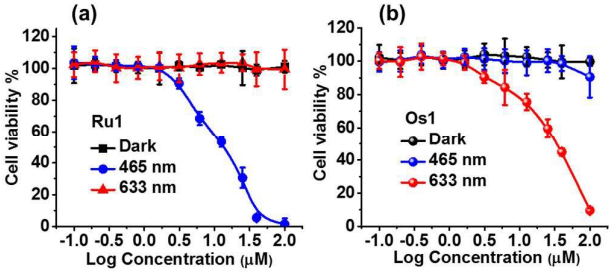

Fig. 4. Growth curves for the A549 cells treated with (a) **Ru1** (b) **Os1** for 4 h in the dark or followed by irradiation with 465 nm (4.8 mW/cm^2, 1 h) or 633 nm light (11.1 mW/cm^2, 3 h). The cells transferred to fresh medium, then incubated for a further 44 h.

Conclusions

We present the first application of an Os(II) polypyridyl complex for lysosome NIR imaging in the living cells. In contrast to its Ru(II) analogue and most of iridium complexes, **Os1** exhibited NIR emission centred around 736 nm, which is usefully situated inside the biological window and out of the range of cellular autofluorescence. Interestingly, we observed that **Os1** accumulated in lysosome with NIR emission, whereas **Ru1** located in mitochondria with red luminescence. Furthermore, **Os1** exhibited more significant phototoxicity towards the cancer cells than **Ru1** upon 633 nm light irradiation. Overall, this study shows that Os(II) polypyridyl complex may offer an useful addition to the growing repertoire of NIR imaging and NIR photodynamic therapy.

We appreciate the financial support of the National Natural Science Foundation of China (NSFC, 21701113) and the Science and Technology Foundation of Shenzhen (JCYJ20170302144346218) for PZ, the NSFC (21471164 and 21525105) and the 973 program (2015CB856301) for HC, the NSFC (21374064, 21471101 and 21671137) and the Foundation for Emerging Industries of Strategic Importance of Shenzhen (JCY20150324140036843) for QZ.

View Article Online
DOI: 10.1039/C7CC07776A

Conflicts of interest

There are no conflicts to declare.

Notes and references

1 (a) Q. Zhao, C. H. Huang and F. Y. Li, *Chem. Soc. Rev.,* 2011, **40,** 2508; (b) V. Venkatesh, N. K. Mishra, I. Romero-Canelón, R. R. Vernooij, H. Shi, J. P. Coverdale, A. Habtemariam, S. Verma and P. J. Sadler, *J. Am. Chem. Soc.*, 2017, **139,** 5656; (c) E. Baggaley, J. A. Weinstein and J. A. G. Williams, *Coord. Chem. Rev.,* 2012, **256,** 1762; (d) P. Zhang, C. K. C. Chiu, H. Huang, Y. P. Y. Lam, A. Habtemariam, T. Malcomson, M. J. Paterson, G. J. Clarkson, P. B. O'Connor, H. Chao and P. J. Sadler, *Angew. Chem. Int. Ed.*, 2017, **56,** DOI: 10.1002/ange.201709082; (e) M. Dickerson, Y. Sun, B. Howerton and E. C. Glazer, *Inorg. Chem.,* 2014, **53,** 10370; (f) P. Zhang, Y. Wang, W. Huang, Z. Zhao, H. Li, H. Wang, C. He and Q. Zhang, *Sensor Actuat. B-Chem.,* 2018, **255,** 283; (g) P. Zhang, W. Huang, Y. Wang, H. Li, C. Liang, C. He, H. Wang and Q. Zhang, *Inorg. Chim. Acta,* 2017, **454,** 240; (h) J. Liu, C. Jin, B. Yuan, X. Liu, Y. Chen, L. Ji and H. Chao, *Chem. Commun.,* 2017, **53,** 2052; (i) L. J. Liu, W. Wang, S. Y. Huang, Y. Hong, G. Li, S. Lin, Z. W. Cai, H. M. D. Wang, D. L. Ma and C. H. Leung, *Chem. Sci.*, 2017, **8,** 4756; (j) K. Q. Qiu, H. Y. Huang, B. Y. Liu, Y. K. Liu, Z. Y. Huang, Y. Chen, L. N. Ji and H. Chao, *ACS Appl. Mater. Interfaces*, 2016, **8,** 12702; (k) L. He, Y. Li, C. P. Tan, R. R. Ye, M. H. Chen, J. J. Cao, L. N. Ji and Z. W. Mao, *Chem. Sci.*, 2015, **6,** 5409; (l) H. J. Zhong, L. H. Lu, K. H. Leung, C. C. L. Wong, C. Peng, S. C. Yan, D. L. Ma, Z. W. Cai, H. M. D. Wang and C. H. Leung, *Chem. Sci.*, 2015, **6,** 5400; (m) D. L. Ma, S. Lin, K. H. Leung, H. J. Zhong, L. J. Liu, D. S. H. Chan, A. Bourdoncle, J. L. Mergny, H. M. D. Wang and C. H. Leung, *Nanoscale*, 2014, **6,** 8489.

2 (a) J. K. Barton, E. D. Olmon and P. A. Sontz, *Coord. Chem. Rev.,* 2011, **255,** 619; (b) Y. J. Liu, C. H. Zeng, H. L. Huang, L. X. He and F. H. Wu, *Eur. J. Med. Chem*., 2010, **45,** 564; (c) M. R. Gill and J. A. Thomas, *Chem. Soc. Rev.,* 2012, **41,** 3179; (d) B. Pena, R. Barhoumi, R. C. Burghardt, C. Turro and K. R. Dunbar, *J. Am. Chem. Soc.,* 2014, **136,** 7861; (e) C. Liu, C. Yang, L. Lu, W. Wang, W. Tan, C. H. Leung and D. L. Ma, *Chem. Commun.*, 2017, **53,** 2822.

3 (a) A. F. A. Peacock and P. J. Sadler, *Chem. Asian J.,* 2008, **3,** 1890; (b) J. Maksimoska, D. S. Williams, G. E. Atilla-Gokcumen, K. S. Smalley, P. J. Carroll, R. D. Webster, P. Filippakopoulos, S. Knapp, M. Herlyn and E. Meggers, *Chem. Eur. J.,* 2008, **14,** 4816; (c) M. Hanif, A. A. Nazarov, C. G. Hartinger, W. Kandioller, M. A. Jakupec, V. B. Arion, P. J. Dyson and B. K. Keppler, *Dalton Trans.,* 2010, **39,** 7345; (d) S. H. van Rijt, A. Mukherjee, A. M. Pizarro and P. J. Sadler, *J. Med. Chem.,* 2010, **53,** 840; (e) L. J. Liu, W. Wang, T. S. Kang, J. X. Liang, C. Liu, D. W. J. Kwong, V. K. W. Wong, D. L. Ma and C. H. Leung, *Sci. Rep.,* 2016, **6,** 36044; (f) C. Yang, W. Wang, G. D. Li , H. J. Zhong, Z. Z. Dong and C. Y. Wong, *Sci. Rep.,* 2017, **7,** 42860.

4 (a) R. G. Alabau, M. A. Esteruelas, M. Oliván and E. Oñate, *Organometallics,* 2017, **36,** 1848; (b) W. K. Chu, S. M. Yiu and C. C. Ko, *Organometallics,* 2014, **33,** 6771.

5 (a) S. Lazic, P. Kaspler, G. Shi, S. Monro, T. Sainuddin, S. Forward and L. Lilge, *Photochem. Photobiol.,* 2017, **93,** 1248; (b) E. C. Glazer, *Photochem. Photobiol.,* 2017, **93,** 1326.

6 (a) B. Durham, J. L. Walsh, C. L. Carter and T. J. Meyer, *Inorg. Chem.,* 1980, **19,** 860; (b) R. S. Lumpkin, E. M. Kober, L. A. Worl, Z. Murtaza and T. J. Meyer, *J. Phys. Chem.,* 1990, **94,** 239.

7 (a) Z. Guo, S. Park, J. Yoon and I. Shin, *Chem. Soc. Rev.,* 2014, **43,** 16; (b) C. Y. S. Chung, S. P. Y. Li, M. W. Louie, K. K. W. Lo and V. W. W. Yam, *Chem. Sci.,* 2013, **4,** 2453.

8 (a) G. Hong, A. L. Antaris and H. Dai, *Nat. Biomed. Eng.,* 2017, **1,** 0010; (b) V. J. Pansare, S. Hejazi, W. J. Faenza and R. K. Prud'homme, *Chem. Mater.,* 2012, **24,** 812; (c) D. Wu and D. F. O'Shea, *Chem. Commun.,* 2017, **53,** 10804; (d) J. Park, Q. Jiang, D. Feng, L. Mao and H. C. Zhou, *J. Am. Chem. Soc.,* 2016, **138,** 3518.

9 (a) Y. Y. Cheng, G. C. Li, Y. Liu, Y. Shi, G. Gao, D. Wu, J. B. Lan and J. S. You, *J. Am. Chem. Soc.,* 2016, **138,** 4730; (b) S. Kaloyanova, Y. Zagranyarski, S. Ritz, M. Hanulova, K. Koynov, A. Vonderheit, K. Mullen and K. Peneva, *J. Am. Chem. Soc.,* 2016, **138,** 2881; (c) X. Zhao, Y. Li, D. Jin, Y. Z. Xing, X. L. Yan and L. G. Chen, *Chem. Commun.,* 2015, **51,** 11721; (d) H. S. Jung, J. H. Lee, K. Kim, S. Koo, P. Verwilst, J. L. Sessler, C. Kang and J. S. Kim, *J. Am. Chem. Soc*., 2017, **139,** 9972.

10 F. D. Duman, I. Hocaoglu, D. G. Ozturk, D. Gozuacik, A. Kiraz and H. Y. Acar, *Nanoscale*, 2015, **7,** 11352.

11 M. Lin, Y. Zhao, S. Q. Wang, M. Liu, Z. F. Duan, Y. M. Chen, F. Li, F. Xu and T. J. Lu, *Biotechnol. Adv.,* 2012, **30,** 1551.

12 L. Yuan, W. Lin, K. Zheng, L. He and W. Huang, *Chem. Soc. Rev.,* 2013, **42,** 622.

13 (a) J. L. Liao, Y. Chi, S. H. Liu, G. H. Lee, P. T. Chou, H. X. Huang, Y. D. Su, C. H. Chang, J. S. Lin and M. R. Tseng, *Inorg. Chem.*, 2014, **53,** 9366; (b) S. Mardanya, S. Karmakar, D. Mondal and S. Baitalik, *Inorg. Chem.*, 2016, **55,** 3475; (c) J. Wang, S. Sun, D. Mu, J. Wang, W. Sun, X. Xiong, B. Qiao and X. Peng, *Organometallics*, 2014, **33,** 2681.

14 K. Qiu, Y. Liu, H. Huang, C. Liu, H. Zhu, Y. Chen, N. J. Liang and H. Chao, *Dalton Trans.,* 2016, **45,** 16144.

15 H. Huang, P. Zhang, B. Yu, C. Jin, L. Ji and H. Chao, *Dalton Trans.,* 2015, **44,** 17335.

16 H. Huang, B. Yu, P. Zhang, J. Huang, Y. Chen, G. Gasser, L. N. Ji and H. Chao, *Angew Chem. Int. Edit.,* 2015, **127,** 14255.

View Article Online
DOI: 10.1039/C7CC07776A

In comparison to ruthenium(II) complex, osmium(II) complex has great advantages of NIR phosphorescence imaging and NIR photodynamic therapy.